AJAE

Open Access

Vol. 15, No. 1, 2020072, March 2021
doi: https://doi.org/10.5572/ajae.2020.072
ISSN (Online) 2287-1160, ISSN (Print) 1976-6912

Research Article

Development of A Low-cost Simultaneous Low Volume Air Sampler Controlled with Sonic Venturi

Zikrilla Bobamuratovich Alimov[1),2)], **Hikaru Kusakari**[1)], **Tomoaki Okuda**[1),*]

[1)]Department of Applied Chemistry, Faculty of Science and Technology, Keio University, 3-14-1 Hiyoshi, Kohoku-ku, Yokohama 223-8522, Japan
[2)]Uzbek-Japan Innovation Center of Youth at the Tashkent State Technical University, 2B, Universitet street, Tashkent 100095, Uzbekistan

***Corresponding author.**
Tel: +81-045-566-1578
E-mail: okuda@applc.keio.ac.jp.

Received: 29 June 2020
Revised: 23 October 2020
Accepted: 17 February 2021

ABSTRACT This study presents the results of designing a low-cost air sampler for multi-component analysis of $PM_{2.5}$. We developed a multi-channel air sampling device using sonic venturi (critical nozzle) that supplies a constant airflow rate of 16.7 L/min. The constant flow rate is achieved with a backpressure ratio of 0.8 or less with a nozzle diameter of 1.375 mm. The sampler halves the cost of comparable devices and simplifies the hardware by replacing the flow meters with critical nozzles. For quantitative evaluation, we measured the coefficient of variation (CV) of each component simultaneously collected five samples at various particulate matter concentrations. This sampler can use different types of filters such as polytetrafluoroethylene and quartz fiber filter at the same time. Meteorological conditions such as ambient temperature, relative humidity and atmospheric pressure did not seem to affect much the flow rate of the sampler. The CV of multi sample analysis for TSP and $PM_{2.5}$ concentrations in all sampling periods were less than 10%. CV of multi sample analysis for most of the major inorganic elements being within the range of 15% or less shows that the precision is sufficient for reliable measurement. We believe that the low-cost multiple air sampler will be used world-widely, and it can contribute to many researchers in both developed and developing countries.

KEY WORDS $PM_{2.5}$, Low-cost, Multiple simultaneous air sampler, Filter sampling, Critical nozzle, Constant flow rate

1. INTRODUCTION

In the past few decades, the global community has begun to understand the effects of particulate matter (PM) and its relationship to many common diseases (Bonzini *et al.*, 2010). PM is also generated when gaseous chemical species react or interact in the atmosphere. Mainly, PM is classified as PM_{10} (<10 μm; coarse) and $PM_{2.5}$ (<2.5 μm; fine) based on their size of particle diameter. $PM_{2.5}$ fraction represents more than 50% of the total mass of PM_{10} (Kim *et al.*, 2015; Lim *et al.*, 2012). The size of particles is directly linked to health problems, in which fine particles are of greater risk since they can penetrate into lung tissues and ultimately enter the blood stream (Kumar and Gupta, 2015; Huang and Ghio, 2006; Cohen *et al.*, 2005; Kunzli and Tager, 2005; Sharma and Agarwal, 2005).

Numerous studies have shown that inhaled particles cause serious respiratory

diseases (Kim *et al.*, 2015; Cadelis *et al.*, 2014; Correia *et al.*, 2013; Fang *et al.*, 2013; Meister *et al.*, 2012; Atkinson *et al.*, 2010). Because of this, air quality research is prioritized by developed countries (Viana *et al.*, 2006) and many of them are trying to reduce air pollutant emissions by using environmentally friendly and efficient practices in industry. In many developing countries, air pollution is a major problem due to the shortage of funds which does not allow the use of environment-friendly techniques for the disposal of waste and the safe handling of hazardous chemicals (Sabyrbekov and Ukueva, 2019; Sapkota and Bastola, 2017; Treesubsuntorn *et al.*, 2017). Because of this, industries in developing countries are releasing thousands of tons of air polluting PM into the atmosphere (Mannucci and Franchini, 2017).

Moreover, the major disadvantages of conventional aerosol sampling methods such as filtration are: one kind filter is not always good enough to analyze all elements or components simultaneously (Liu *et al.*, 2015; Hinds, 1998). Multi-component analysis requires sampling with several types of filters at the same time. For example, polytetrafluoroethylene (PTFE) is suitable for elemental analysis whereas quartz fiber filter (QFF) is required to analyze carbonaceous species. In this case, the aerosol sampling needs several devices. Measurement and regular monitoring of fine PM in developing countries is extremely important to reduce emissions in the air so that one can understand the sources and formation mechanisms of PM; however, many of the countries with poor economics would not afford to purchase many of highly accurate but expensive sampling analysis devices.

A major aim of the study is to develop a low-cost air sampler to obtain multiple samples at the same time. The multiple samples would allow researchers to carry out a variety of chemical analysis that are requested to conduct multi-component analysis of air pollutants so that one can understand these sources and formation mechanisms. A multiple air sampler is ideal when sampling under identical conditions of temperature and humidity, and over the same period to conduct multi-component analysis of air compositions. Multiple air samplers also require a stable air flow rate to obtain the same sample. However, it is difficult to collect samples under the same conditions using multiple air samplers due to the cost of expensive flow meters and flow control devices. Critical nozzles give advantages such as minimal upstream piping, long term accuracy of flow rate, no mechanical parts, and excellent flow rate repeatability due to unaffected by downstream flow disturbances. Various devices with critical nozzles have been developed to measure low gas flow rates in a calibration facility (Nakao *et al.*, 1996), and Wang *et al.* (1999) presented the multi-point air sampling using a critical nozzle to measure aerosol spatial distribution at multiple points in a room. The sampler, however, is not directed to study outdoor $PM_{2.5}$, instead, it intends to measure indoor aerosol. Besides, there have not been achieved the verification that provided the information of uniformity of the multiple samples collected using those samplers by analyzing the chemical compositions of the obtained samples.

In this paper, we present the design and lab evaluation of a low-cost and simultaneous low volume air sampler controlled with sonic venturi to obtain multiple homogeneous samples at the same time to conduct multi-component analysis of aerosol particles. The sampler allows to obtain multiple homogeneous and heterogeneous (in terms of filter materials) samples at the same time. Also, the device reduces the repairing and operation (running) cost on account of very simple construction. This device will be used extensively in our field researches in various developing locations such as the Central Asian countries.

2. MATERIALS AND METHODS

2.1 Simultaneous Low Volume Air Sampler Development

Schematic drawing and a picture of the constant flow multiple sampler are shown in Fig. 1a and 1b. It consists of impactors to remove particles greater than 2.5 μm of aerodynamic diameter, a filter for collecting $PM_{2.5}$, a critical nozzle for fixing the flow rate, the flow control valve, and a pump. This sampler is named "SilVy-5", a shortening of "Simultaneous low Volume air sampler controlled with Sonic Venturi" and it has five sampling lines. The number of samples is not limited to be five, it can be variable depending on the situation.

Multiple homogeneous and single blank filter holders are connected to one outlet line. Each sampling device includes an impactor for removing coarse particles and a filter for collecting fine particles. The two-stage impactor, which used round jets, was designed for collecting $PM_{2.5}$ at an air flow rate of 16.7 L/min, based on the design in ISO (International Organization for Standardization) and JIS (Japanese Industrial Standards) (JIS Z 8767:2006; ISO 9300:2005). The five filters are provided with an

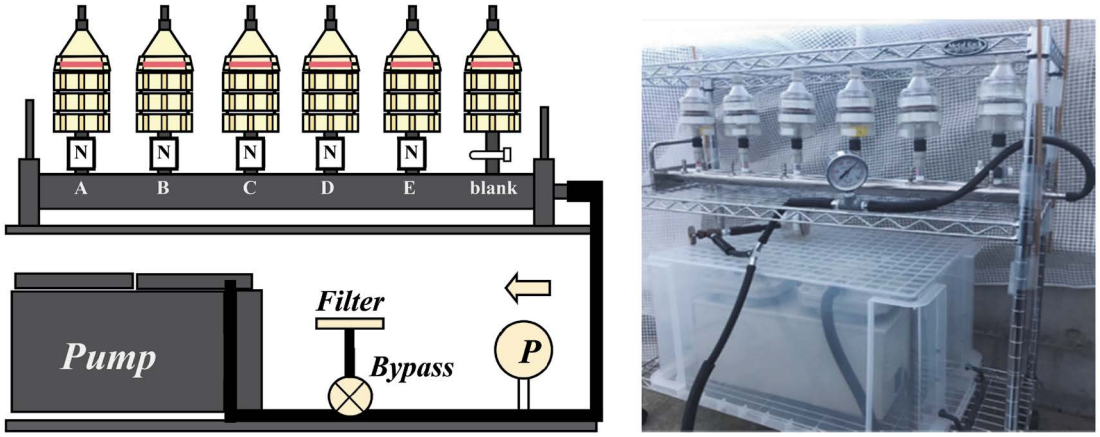

Fig. 1. Schematic drawing (a) and picture (b) of simultaneous low volume air sampler (SilVy-5). P is the pressure measurement gauge and N is the nozzle.

equal airflow rate and the blank filter does not have air flow through it to compare it with the other filters.

2.2 Venturi Sound Nozzle to Control Airflow Rate

2.2.1 Theory

Measurement of the airflow rate is an important issue when using a multiple air filter sampler because the concentration of the air pollutant is determined by the ratio of the sampled components quantity to the sampled air volume. Using a venturi sound nozzle to control airflow rate is considered to be a method that can solve this issue and work long term, after calibration and metering of gas flow meters. It is accurate, simply construction, and inexpensive.

According to the flow continuity equation (1), the flow rate Q is constant, but, the flow velocity u changes depending on the cross-section area $S\,(=\pi d^2/4)$ of the venturi sound nozzle portions (Fig. 2):

$$Q = u_1S_1 = u_2S_2 = \ldots = u_iS_i \tag{1}$$

When the pressure ratio between the upstream (P_1) and downstream (P_2) sides of the nozzle is kept below the critical backpressure ratio (P_c), the flow velocity u at the throat is fixed at the sonic speed a, and the flow rate is constant regardless of the downstream state of the nozzle (Nakamura *et al.*, 2014; Morioka *et al.*, 2011; Wang and Zhang, 1999; Johnson, 1965). P_c is the pressure ratio between critical pressure (P_{cr}) at the throat of the nozzle and downstream (P_2) sides of the nozzle. The flow velocity u at the throat can be expressed as (Wang and Zhang, 1999).

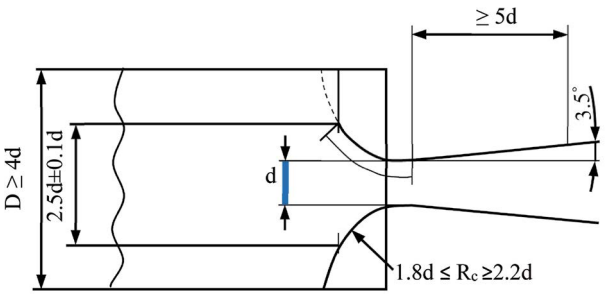

Fig. 2. Schematic sectioned diagram of a venturi sound nozzle (Morioka *et al.*, 2011; JIS Z 8767:2006).

$$u = \sqrt{\frac{2\gamma}{\gamma\text{-}1}\frac{P_{th}}{\rho_1}\left[1-\left(\frac{P_{th}}{P_1}\right)^{(\gamma\text{-}1)/\gamma}\right]} \tag{2}$$

where

P_{th} - the pressure at the throat (Pa);

ρ_1 - air density (kg/m^3);

γ - a specific heat ratio of the gas. Here, $\gamma = 1.4$.

In this case, the constant flow rate depends on a constant upstream condition. The flow velocity is fixed at the sonic speed at the throat portion of the critical nozzle due to the properties of the gas flow at the throat of the nozzle.

The theoretical flow rate Q_{th} passing through the venturi sound nozzle is expressed by the equation (3) based on the flow state quantity in the throat of the nozzle (Morioka *et al.*, 2011):

$$Q_{th} = S_{th} \cdot a^* \cdot \quad (3)$$

where

S_{th} - the throat cross section area (m^2);

a^* - the sound speed at the throat (m/s).

The speed of sound depends on the heat capacity ratio of flowing phase (e.g. Morioka *et al.*, 2011; Younglove and Frederick, 1992; Wong, 1990). The heat capacity ratio expresses the effect of changing temperature, pressure, volume, density, etc. on the properties of the gas or air phases. Younglove and Frederick (1992) measured the speed of sound in the vapor and supercritical phases of air. The results showed that with increasing pressure (in the range 0–4 MPa) the speed of sound decreases, but with increasing temperature the speed of sound increases. The equation (4) holds between the sound speed a_0 at the stagnation point upstream of the nozzle and the sound speed a^* at the throat portion.

$$a^* = \sqrt{\frac{2}{\gamma+1} \times a_0^2} \quad (4)$$

where

γ - a specific heat ratio of the gas. Here, $\gamma = 1.4$;

a_0 - the sound speed in air at atmospheric pressure and room temperature, it is 340 m/s (Amrani, 2013).

The throat portion is in a state of higher pressure, in which the density of compressed air is high, in contrast to the normal state. In a flow path in which the cross-sectional area of the critical nozzle continuously increases or decreases, the flow cannot reach the sonic speed (critical state) in the middle of the flow path. In order for a flow to be sonic in a flow channel, there can only be a subsonic-sonic-supersonic configuration or vice versa.

2.2.2 Design New Nozzle to Control Flow Rate for Environmental Air Sampling

In this study, instead of controlling the flow rate with a flow meter, we manufactured a critical nozzle that fixes the flow rate at 16.7 L/min. The shape of the critical nozzle is based on ISO and JIS (JIS Z 8767:2006; ISO 9300:2005). The standard drafting is as shown in Fig. 2. Since each dimension of the critical nozzle depends on the value of the throat diameter d, the critical nozzle shape can be determined as long as the throat diameter is known. The nozzle was manufactured with a throat diameter between $1.30 \leq d \leq 1.38$. The experiments were conducted to determine the impacts of meteorological conditions (temperature and humidity) and filters materials (Polytetrafluoroethylene (Cytiva's Whatman 7592-104, $PM_{2.5}$ PTFE membrane filter, 46.2 mm, pore size 2 μm), polycarbonate (Toyo Roshi Kaisha, Ltd, Advantec K020A047A membrane filter, 47 mm, pore size 0.2 μm), quartz fiber (Toyo Roshi Kaisha, Ltd, Advantec QR-100, 47 mm, Collection Efficiency 99.99% for 0.3 μm DOP), glass fiber (Toyo Roshi Kaisha, Ltd, Advantec GA-100, 47 mm, Collection Efficiency 96% for 0.3 μm DOP), and nitrocellulose (MF-Millipore AAWP04700 membrane filter, 47 mm, pore size 0.8 μm), on the flow rate.

The experimental system for setting the fixed flow rate is shown in Fig. 3. An experiment was conducted to confirm the backpressure ratio of all manufactured critical nozzles. When the valve was opened, the suction power of the pump gradually increased, and the pressure on the outlet side of the nozzle decreased to confirm the backpressure coefficient (backpressure coefficient), at which the flow rate became constant.

2.3 Collection Samples of TSP and $PM_{2.5}$

2.3.1 Sampling

Five TSP (total suspended particles) and $PM_{2.5}$ samples were simultaneously collected using the SilVy-5. The control (blank) sample was also set into another fil-

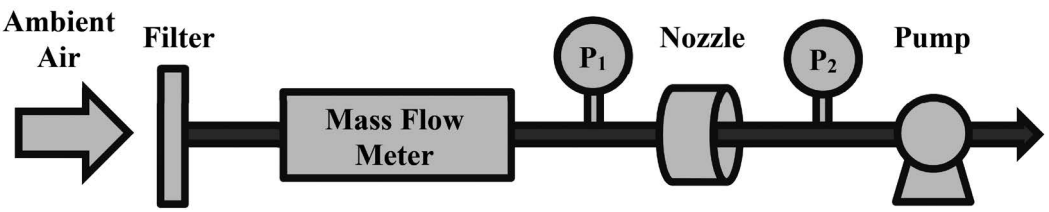

Fig. 3. Schematic diagram of the experimental setup for confirming the back-pressure ratio of the nozzle. Mass flow meter: AZbil CMS0050 calibrated at 20°C and 1 atm. Pump: ULVAC diaphragm dry vacuum pump DA-120S. P_1 and P_2 are the pressures before (upstream pressure) and after (downstream pressure) the nozzle, respectively.

ter holder without any air flow through the filter. TSP and $PM_{2.5}$ were collected on PTFE filters (same product for $PM_{2.5}$ sampling). We used impactors by placing a donut filter between the nozzle plate and impaction plate to collect particles larger than 2.5 μm, which let $PM_{2.5}$ particles be collected on the sampling filters.

The sampler was located on the laboratory balcony on the 5th floor of a building at Yagami campus of Keio University in Yokohama, Japan. TSP was also collected during 72 hours in the following three sampling periods: 2020/08/21–24, 2020/08/24–27, 2020/08/28–31 and 24 hours in three sampling periods: 2020/09/02–03, 2020/09/03–04, and 2020/09/14–15. $PM_{2.5}$ was collected during 72 hours in the following three sampling periods: 2019/11/25–28, 2019/11/29–12/2, and 2019/12/8–11. The air flows rate for TSP and $PM_{2.5}$ samplings was fixed at 16.7 L/min through each A, B, C, D, and E impactors and 0 L/min for the control. The flow rate (with impactor, but without filters) was checked before and after sampling, and it was confirmed that the flow rate was always fixed at 16.7 ± 0.1 L/min at all the inlets. The backpressure ratio was adjusted using the bypass so that it was always maintained at 0.70 ± 0.04, which was below the critical backpressure ratio.

2.3.2 Determine of Mass Concentration by Weighing Method

Mass concentration was determined by following the official method (JIS Z 8851:2008). Weighing was carried out by electric balance Sartorius ME235S (resolution $d = 0.01$ mg) in room temperature 24 ± 3°C, and relative humidity $< 35\%$. Arithmetic mean of field blank ($n = 3$–5) was subtracted from sample weight.

2.3.3 Elemental Analysis by X-ray Fluorescence Analysis (XRF)

The collected filter samples were placed in a clean polystyrene case, sealed in a polyethylene bag, stored refrigerated (4°C or below), and analyzed within one week after the samples were collected. The samples were subjected to mass concentration measurement and inorganic element analysis using Energy dispersive X-ray fluorescence analysis (EDXRF) (EDXL300, manufactured by Rigaku Corporation) (Okuda *et al.*, 2014). EDXL300 allows the users to achieve standardless analysis that we do not need to prepare standard materials of each target element due to the device has a powerful fundamental parameter (FP) algorithm. In FP method, many parameters are considered in the calculations such as the interaction and absorption between photons and atoms, the thickness of the atomic layer, the elemental compositions. SRM2783 (Air Particulate on Filter Media, provided by NIST) was analyzed daily to check the instrument condition.

3. RESULTS AND DISCUSSION

3.1 Constant Flow Rate Performance of the Critical Nozzles

The critical backpressure coefficient P_c changes according to the Reynolds number, which greatly depends on the shape of the critical nozzle, the viscosity of the fluid, and a value unique to the nozzle. Therefore, the value P_c is an important variable that must be confirmed experimentally. Before a critical nozzle is used for controlling the flow rate, the critical backpressure coefficient needs to be checked to confirm that the airflow in the nozzle transitions to a critical state. When the air is drawn through a filter, the flow rate will be constant, if the pressure ratio between the upstream (P_1) and downstream (P_2) sides of the nozzle is kept below the critical backpressure ratio (P_c). When the backpressure ratio (P_2/P_1) becomes 0.8 or less, the flow rate is fixed and steady.

In this study, instead of controlling the flow rate with a flow meter, we used a critical nozzle that fixes the flow rate at 16.7 L/min. Controlling the flow rate by critical nozzle heavily depends on the throat diameter of the critical nozzle and the backpressure of the flow. We conducted experiments to confirm the constant flow rate of air in the throat diameter range of 1.30 mm to 1.38 mm. The results of the experiments are shown in Figs. 4 and 5. In

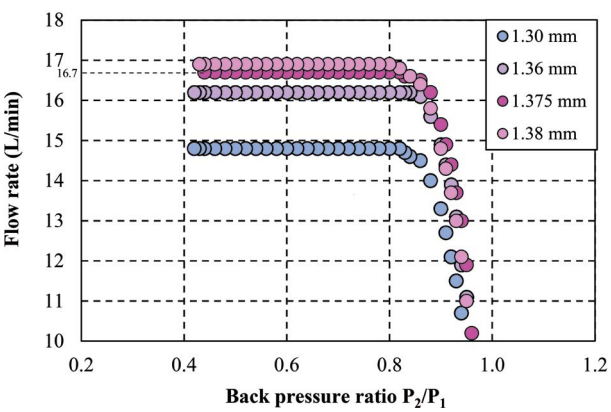

Fig. 4. Relationship between backpressure ratio and flow rate for the different nozzle diameters.

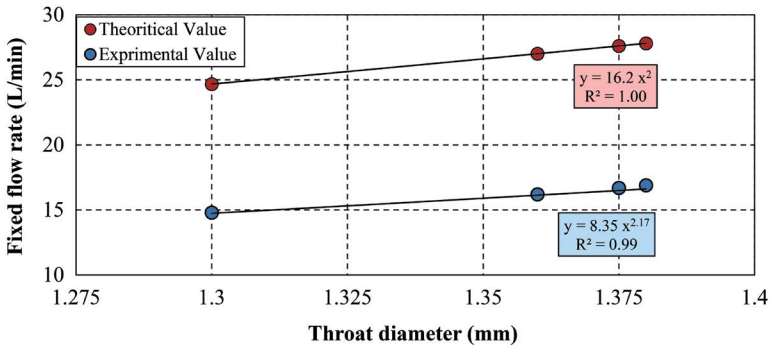

Fig. 5. Relationship between throat diameter and fixed flow rate.

Table 1. Cross-sectional area, boundary layer thickness and percentage of boundary layer for each throat diameter.

Throat diameter (x) (mm)	Cross-sectional area (mm^2)	Effective area of sound speed (mm^2)	Boundary layer thickness (mm)	Percentage of the boundary layer (%)
1.30	1.33	0.718	0.344	26.4
1.36	1.45	0.786	0.359	26.4
1.375	1.48	0.805	0.362	26.3
1.38	1.49	0.820	0.358	25.9

the range of the aforementioned nozzle throat diameters, it was found that a constant flow rate fluctuated from 14.8 L/min to 16.9 L/min. In this case, when the back pressure ratio becomes 0.8 or less, the flow rate is stable. An unstable flow rate was observed when the back-pressure ratio was higher than 0.8 for all nozzle diameters.

Fig. 5 shows the relationship between the throat diameter of the critical nozzles and the fixed flow rate. Here, the theoretical value of the fixed flow rate equals 310 m/s at the throat portion at room temperature in the cross-sectional area. From the experiment, it was found that when the throat diameter d was in the range of $1.30 \leq d \leq 1.38$, the relationship between the throat diameter and the fixed flow rate was approximated by $y = 8.35x^{2.17}$, which was 0.65 times lower than the theoretical value. The discrepancy between the theoretical value and the experimental value was quite large. It was questioned whether the flow velocity at the throat in the critical nozzles did not reach sonic speed. Therefore, in this case, it is necessary to deepen the discussion quantitatively on the fixed flow rate at the throat.

Assuming that the theoretical value of the speed of sound at a fixed flow rate holds, the boundary layer that develops inside the actual nozzle is considered to be the cause of the difference between the theoretical value and the experimental value. When the throat portion is compressed, the air density reaches its maximum. Therefore, the flow velocity at the throat is fixed at the sonic speed at the throat portion of the critical nozzle due to the nature of the gas flow, and the flow rate remains constant regardless of the downstream state of the nozzle. In this case, the constant flow rate depends on a constant upstream condition. The speed of sound changes depending on the flow density, that is to say, when flow density decreases, the speed of sound increases.

Table 1 summarizes the throat diameter, cross-sectional area, effective area (experimental value of fixed flow rate/sonic speed), thickness of the boundary layer, and ratio of the boundary layer for each throat diameter. The ratio of the boundary layer to the throat diameter is about $26 \pm 1\%$, which agreed well with a simulation result reported by Alam *et al.* (2016). Therefore, it is determined that the critical nozzle we used has reached the sound speed at the throat portion.

According to experimental results, the constant air flow rate at 16.7 L/min requires a backpressure ratio of 0.8 or less with a nozzle diameter of 1.375 mm. A critical nozzle with the same property as shown in Fig. 6 was prepared and used in the experiment.

Studying the effect of meteorological conditions on

the flow rate through the passed nozzle is most important because, in many regions, the temperature and humidity vary with rapid differences. Fig. 7 represents the relationship between the flow rate and weather conditions. The flow rates of sampling lines under the meteorological conditions of ambient temperature ranged from a minimum of 16.0°C to a maximum of 32.7°C and the humidity ranged from 32% to 88%. The maximum flow rate was observed 17.3 L/min at 16.5°C and the minimum flow rate was 16.7 L/min at atmospheric temperatures ranging from 25°C to 32.7°C. The flow rate was

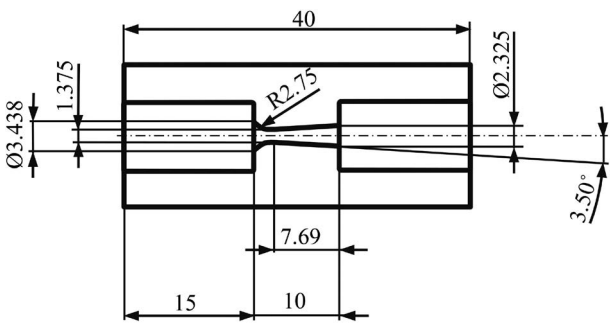

Fig. 6. Design and sizes (mm) drawing of critical nozzle with fixed flow rate of 16.7 L/min.

17.1 L/min at 16.0°C (and 1017.1 hPa) and 17.3 L/min at 16.5°C (and 1021.5 hPa) possibly due to the higher upstream (atmospheric) pressure. Atmospheric pressure varied from 1006 hPa to 1021.5 hPa in measuring the flow rate. When the temperatures were almost equal, the pressure changed the flow rate to 0.1–0.2 L/min. During experiments, the exact correlation was not observed between the flow rate and the atmospheric pressure because the variation of the atmospheric pressure was low. The humidity did not significantly affect the flow rate. The experiments showed that high temperature slightly reduces the flow rate, but the relationship is not significant. It means that the flow rate is almost constant at the observed range of ambient air temperature. The impacts of temperature may depend on the compressibility of the air passing passes through the nozzle throat and the pressure increases. In the past study (Johnson, 1965), the compressibility is given as a function of density and temperature for air and steam, it is necessary to develop the mass-flow-rate solution. There is defined the pressure-density-temperature relation is given by

$$Q_{th} = C_{th}^{*} \frac{P_o}{\sqrt{RT_o}} \tag{5}$$

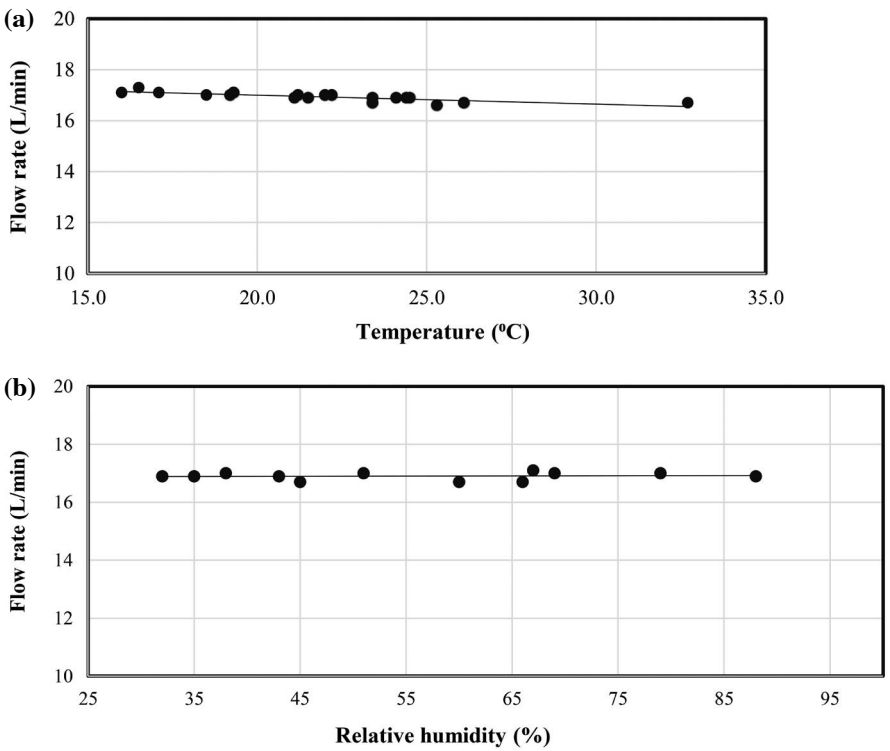

Fig. 7. The impacts of temperature (a) and humidity (b) on the flow rate through passing the nozzle.

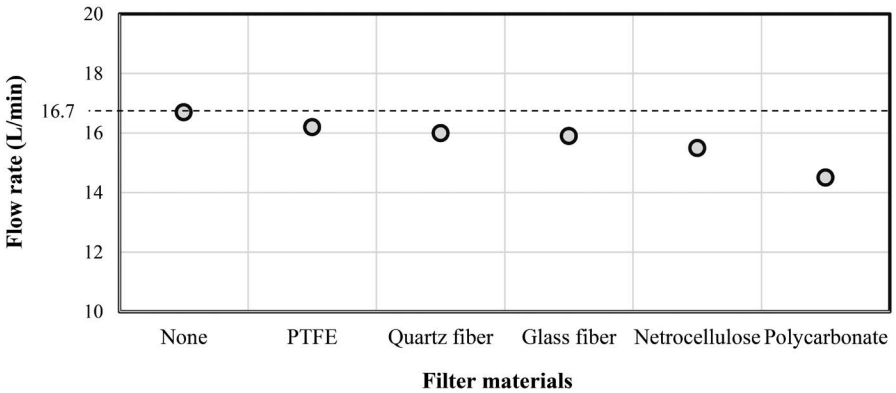

Fig. 8. The impacts of filter materials on the flow rate through passing the nozzle.

where

C^*_{th} - the ideal-gas critical-flow factor;
P_o - the stagnation pressure (Pa);
R - ideal gas constant;
T_o - stagnation temperature (K).

The ideal-gas critical-flow factor defined by

$$C^*_{th} = \left[\gamma \left(\frac{2}{\gamma+1}\right)^{\frac{\gamma+1}{\gamma-1}}\right]^{1/2} \frac{P_o}{\sqrt{RT_o}} \quad (6)$$

The equation (5) shows that the upstream pressure (P_1) changes the flow rate. The flow resistance of filters reduces the upstream pressure between the filter and nozzle. Fig. 8 shows the experimental results for determining the flow rate resistances of different filter materials. The resistance decreased the flow rate passing through nozzles up to 14.5 L/min. The highest value of pressure loss passing through filters belongs to the polycarbonate filter and, the smallest belongs to the PTFE filter. When user want to keep the flow rate in the ±5% range for 16.7 L/min (15.9–17.5 L/min), one can use the filters made of PTFE, quartz or glass fiber.

It is known that the penetration of the impactors changes related to the flow rate (Okuda *et al.*, 2015). Fig. 9 shows the results of experiments to determine the 50% cut-off diameter for the impactor (range, 12 to 20 L/min) and the USEPA WINS $PM_{2.5}$ impactor (at 16.7 L/min). The 50% cut-point of the impactor for ambient aerosols at an air flow rate of 14.5–18.0 L/min meets the JIS Z8851:2008 (2.5 ± 0.2 μm), and that for WINS $PM_{2.5}$ impactor at 16.7 L/min was 2.46 μm. Therefore, $PM_{2.5}$ separation was practically achieved well for all types of filters examined in this study.

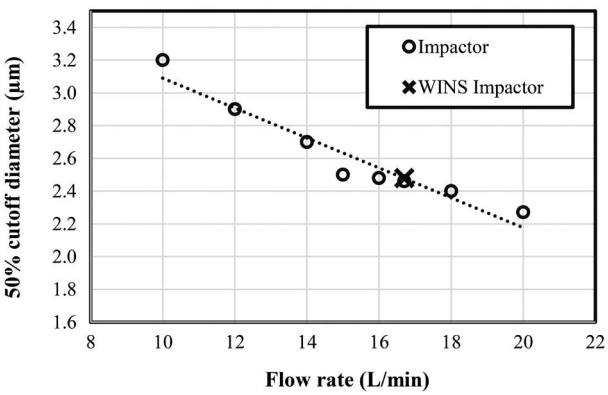

Fig. 9. Penetration curves for the impactor at different flow rate, and for the USEPA WINS $PM_{2.5}$ impactor (@16.7 L/min).

3.2 Evaluation of SilVy-5 by TSP and $PM_{2.5}$ Sample Collection Performance

Evaluation of SilVy-5 has been carried out by calculating mass loading values on the filter during sampling periods and element concentration analyzing of TSP and $PM_{2.5}$ samples. TSP samples were collected in the 2020/08/21–24, 2020/08/24–27, and 2020/08/28–31 periods for 72 hours. The concentrations of TSP in the air were 19.4 ± 0.5 μg/m^3, 21.7 ± 0.3 μg/m^3, and 14.4 ± 0.2 μg/m^3, respectively. TSP samples were also collected in the 2020/09/02–03, 2020/09/03–04, and 2020/09/14–15 periods for 24 hours. The concentrations of TSP in the air were 8.1 ± 0.4 μg/m^3, 5.8 ± 0.3 μg/m^3, and 6.2 ± 0.3 μg/m^3, respectively. Table 2 shows that CV for TSP concentrations are from 1.5 to 2.5% for 72 hours sampling, and from 4.9 to 5.2% for 24 hours sampling, respectively. The CV for TSP concentrations in all sampling periods were less than 15% of the target value,

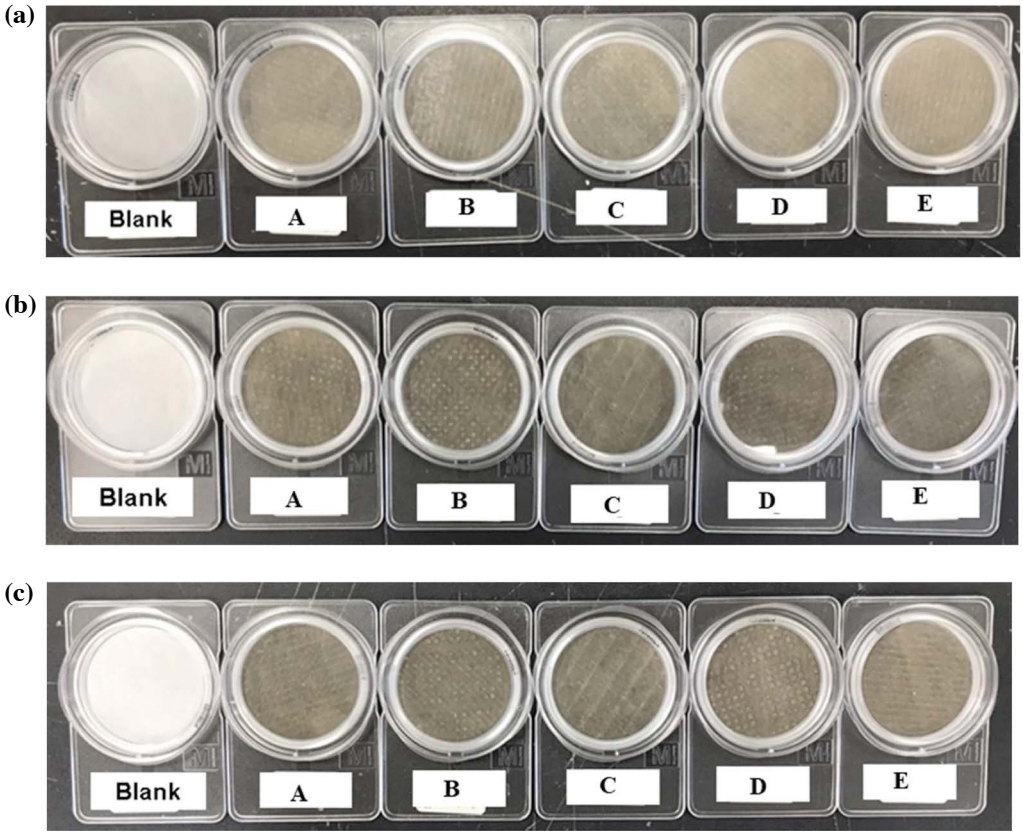

Fig. 10. Pictures of filter samples and blank after collection (mean value of the concentrations of $PM_{2.5}$ in the air): (a) 2019/11/25–28 (6.6 μg/m^3); (b) 2019/11/29–12/2 (10.4 μg/m^3); (c) 2019/12/8–11 (9.8 μg/m^3). The diameters of the filters are 46.2 mm.

Table 2. Measured TSP and $PM_{2.5}$ sample mass concentration and reference value (μg/m^3).

Sampling periods	Sample	Sampling time (hours)	Reference value*	Measured value						
				1	2	3	4	5	Mean ± SD	CV (%)
2020/08/21–24	TSP	72		20.1	19.0	19.0	19.7	19.2	19.4 ± 0.5	2.5
2020/08/24–27	TSP	72		21.3	21.5	22.1	21.6	21.9	21.7 ± 0.3	1.5
2020/08/28–31	TSP	72		14.3	14.2	14.1	14.7	14.5	14.4 ± 0.2	1.7
2020/09/02–03	TSP	24		8.5	8.3	7.8	8.1	7.5	8.1 ± 0.4	4.9
2020/09/03–04	TSP	24		5.9	6.0	5.7	6.2	5.4	5.8 ± 0.3	5.2
2020/09/14–15	TSP	24		6.4	6.2	6.0	6.6	5.8	6.2 ± 0.3	5.2
2019/11/25–28	$PM_{2.5}$	72	7.7	6.2	6.7	7.1	6.2	7.0	6.6 ± 0.4	6.5
2019/11/29–12/2	$PM_{2.5}$	72	11.4	10.0	10.5	10.4	10.4	10.9	10.4 ± 0.3	3.1
2019/12/8–11	$PM_{2.5}$	72	9.5	10.8	9.3	9.2	9.2	10.6	9.8 ± 0.8	8.3

*$PM_{2.5}$ concentration value at Nakahara Ward Office, Kawasaki City Government (NWOKCG, 2020).

which recommended by Ministry of the Environment, Government of Japan (MOEGJ, 2019). $PM_{2.5}$ samples collected in the 2019/11/25–28, 2019/11/29–12/2, and 2019/12/8–11 sampling periods for 72 hours, the concentrations of $PM_{2.5}$ in the air were 6.6 ± 0.4 μg/m^3, 10.4 ± 0.3 μg/m^3, 9.8 ± 0.8 μg/m^3, respectively. The images of the blank and sample filters of $PM_{2.5}$ are shown in Fig. 10, and element analysis results for $PM_{2.5}$ and TSP are shown in Fig. 11. Table 2 shows that the CVs for $PM_{2.5}$ concentrations were between 3.1% and 8.3% that

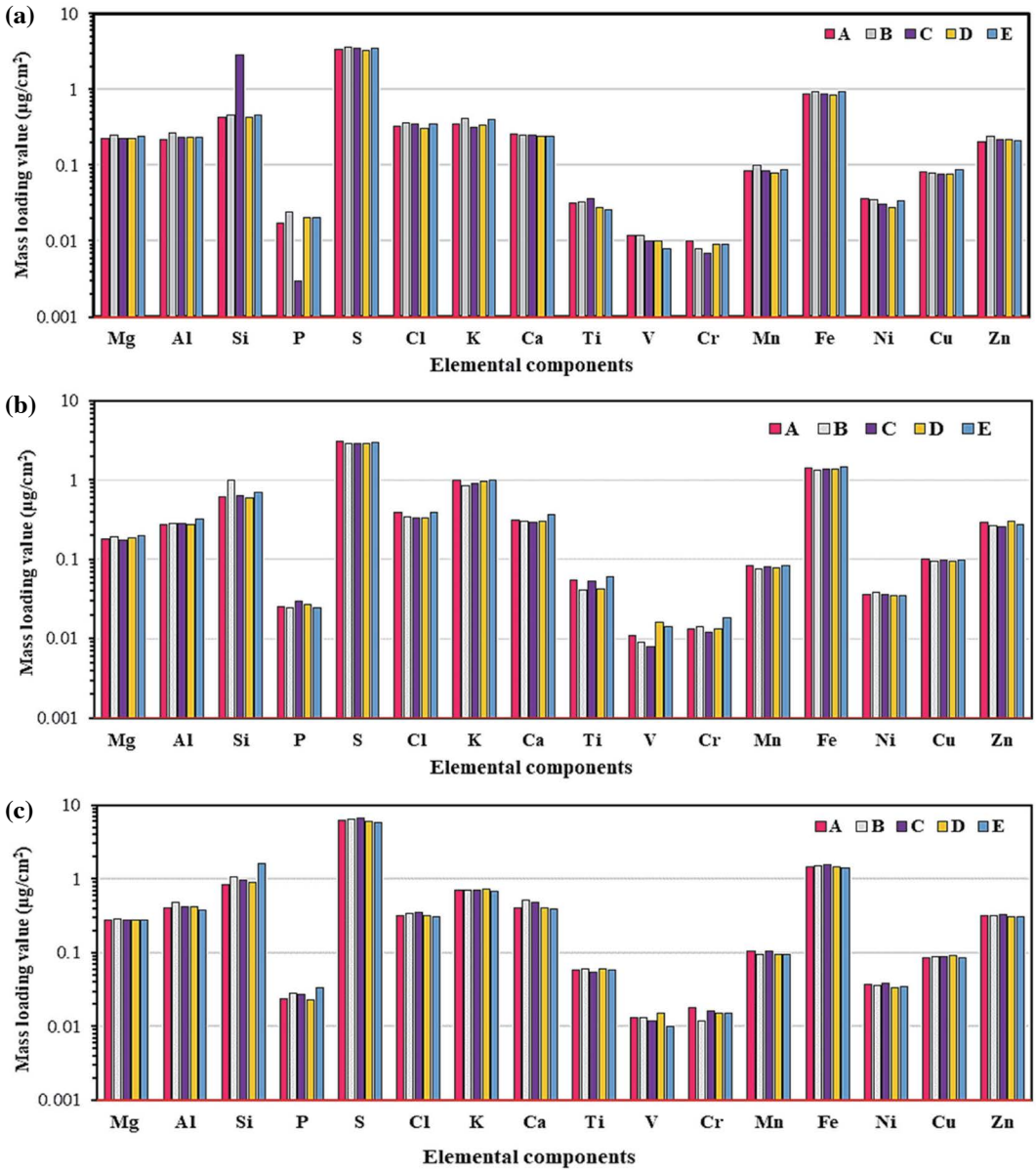

Fig. 11. Inorganic element analysis results for $PM_{2.5}$ samples: (a) 2019/11/25–28; (b) 2019/11/29–12/2; (c) 2019/12/8–11 and for TSP samples: (d) 2020/09/02–03; (e) 2020/09/03–04; (f) 2020/09/14–15. The legends A, B, C, D, E are the identification letters of sample holder in a sampler.

were less than 15%. The reference values in the 2020/08/21–24, 2020/08/24–27, and 2020/08/28–31 periods were 7.7 μg/m^3, 11.4 μg/m^3, and 9.5 μg/m^3, respectively. In the data displayed in Table 2, it can be seen that the difference between the concentrations of $PM_{2.5}$ and the reference values were between 3% and 14%. In the sampling periods, the $PM_{2.5}$ concentration values were obtained for Nakahara Ward Office, Kawasaki City Government (located about 2.2 km from the sampling location) (NWOKCG, 2020).

Fig. 12 show the coefficient of variation (CV) for each average elemental mass loading values in all filters. For quantitative evaluation of three sampling periods, CV of each component concentration of five samples of TSP and $PM_{2.5}$ was calculated and the variation is summarized in Table 3. The inorganic element components analysis of TSP and $PM_{2.5}$ showed that the major components are Mg, Al, Si, S, Cl, K, Ca, Fe, and Zn. The mass

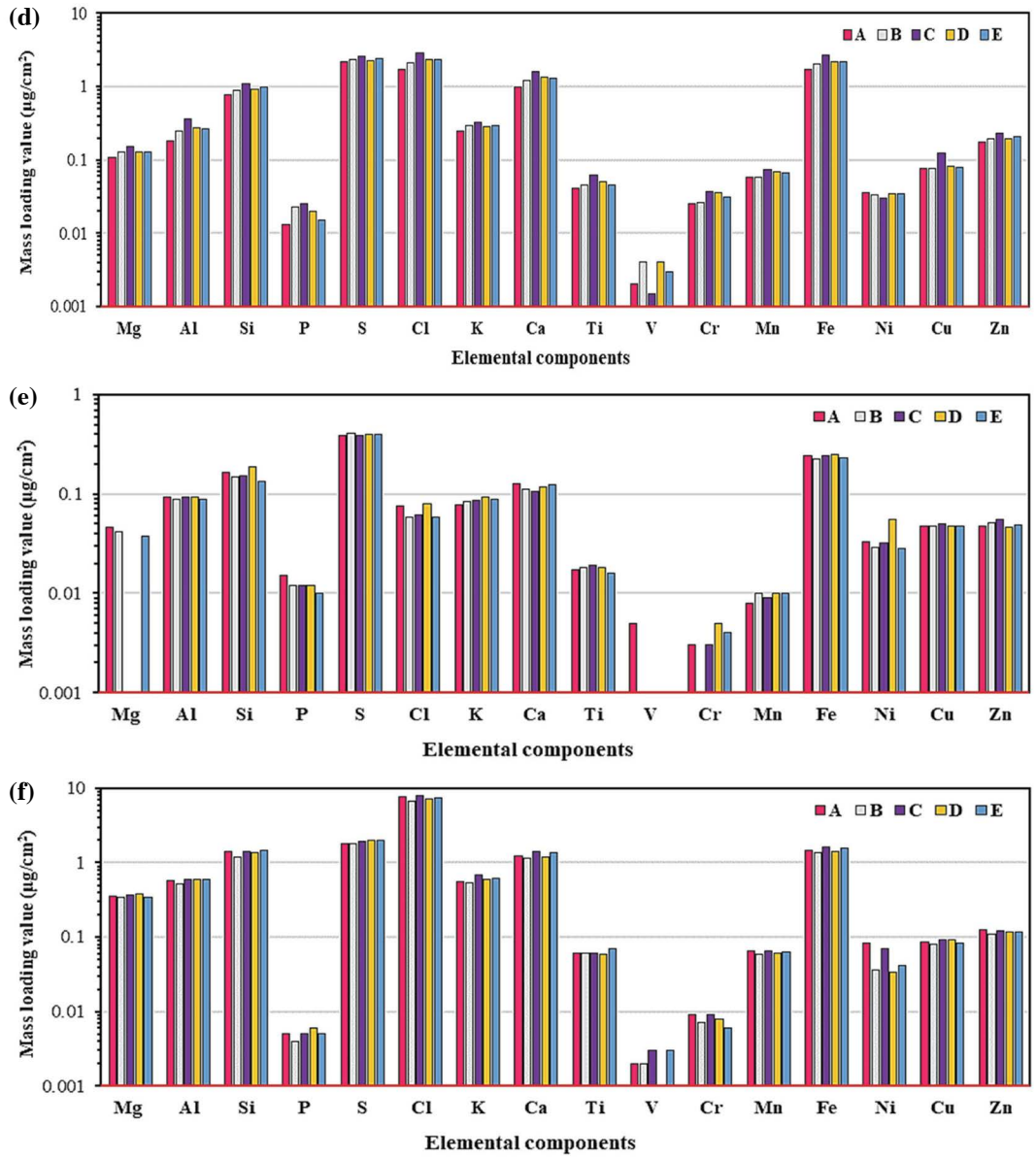

Fig. 11. Continued.

loading values on filter and concentrations of the components in the air are higher than 100 ng/cm^2 and 20 ng/m^3, respectively. Also, in the comparison of the samples obtained over the three sampling periods for TSP, and $PM_{2.5}$ the composition of inorganic elements were quite similar.

In general, it is said that desirable deviation from arithmetic mean for duplicate analysis is within ±15% (MOEGJ, 2019). In the collected samples of TSP, the CVs of Mg, Si, S, K, Mn, Ni, and Zn were less than 15%, Cl, Ca, Ti, Cr, and Fe were between 15–20% and Al, P, V, and Cu were greater than 20% in 2020/09/02–03 sampling period, all the other elements besides Cl, Cr, and Ni was less than 15% in 2020/09/03–04 and only V, Cr, Ni exceed 15% in 2020/09/14–15. Similarly, the CVs for mass loading value on filter of Mg, Al, S, Cl, K, Ca, Mn, Fe, Ni, Cu and Zn were less than 15% for a concentration larger than 30 ng/cm^2 in the three sampling periods for $PM_{2.5}$, CV for V was 16.1% in 2019/11/25–28 and CV for Ti, V, Cr were between 16.1–29% for a concentration lower than 50 ng/cm^2 in 2019/11/29–12/2. The CV of Si in the $PM_{2.5}$ samples collected in the three sampling

Table 3a. The mass loading values on the filter and CV for each elements of TSP. The target of CV value is fixed 15% (MOEGJ, 2019).

Sampling period	2020/09/02–03		2020/09/03–04		2020/09/14–15		PTFE blank filter (n = 15) (μg/cm²)
Element	Mean ± SD (μg/cm²)	CV (%)	Mean ± SD (μg/cm²)	CV (%)	Mean ± SD (μg/cm²)	CV (%)	
Mg	0.130 ± 0.016	12.3	0.042 ± 0.005	10.8	0.355 ± 0.016	4.5	n.d.–0.0026
Al	0.265 ± 0.064	24.1	0.091 ± 0.002	2.6	0.578 ± 0.033	5.8	0.021–0.039
Si	0.926 ± 0.118	12.7	0.158 ± 0.020	12.6	1.362 ± 0.098	7.2	0.003–0.012
P	0.019 ± 0.005	26.7	0.012 ± 0.002	14.7	0.005 ± 0.001	14.1	0.001–0.003
S	2.356 ± 0.157	6.6	0.395 ± 0.010	2.0	1.912 ± 0.107	5.6	0–0.001
Cl	2.289 ± 0.428	18.7	0.067 ± 0.010	15.4	7.322 ± 0.448	6.1	n.d.
K	0.288 ± 0.026	9.0	0.086 ± 0.006	7.0	0.595 ± 0.054	9.1	n.d.–0.015
Ca	1.281 ± 0.219	17.1	0.117 ± 0.009	7.3	1.278 ± 0.109	8.5	0.01–0.032
Ti	0.049 ± 0.008	16.5	0.018 ± 0.001	6.5	0.062 ± 0.005	7.5	n.d.–0.007
V	0.003 ± 0.001	39.3	0.005	–	0.003 ± 0.001	23.1	n.d.
Cr	0.031 ± 0.006	17.8	0.004 ± 0.001	25.5	0.008 ± 0.001	16.7	n.d.–0.004
Mn	0.065 ± 0.008	11.6	0.009 ± 0.001	9.5	0.062 ± 0.003	4.6	n.d.
Fe	2.161 ± 0.339	15.7	0.238 ± 0.009	3.7	1.485 ± 0.107	7.2	0.013–0.022
Ni	0.034 ± 0.002	6.9	0.036 ± 0.012	32.6	0.052 ± 0.022	41.5	n.d.–0.041
Cu	0.088 ± 0.020	22.7	0.048 ± 0.001	2.8	0.087 ± 0.004	5.0	0.031–0.041
Zn	0.201 ± 0.019	9.4	0.050 ± 0.004	7.2	0.119 ± 0.007	5.5	n.d.–0.028

Table 3b. The mass loading values on the filter and CV for each elements of $PM_{2.5}$. The target of CV value is fixed 15% (MOEGJ, 2019).

Sampling period	2019/11/25–28		2019/11/29–12/2		2019/12/8–11		PTFE blank filter (n = 15) (μg/cm²)
Element	Mean ± SD (μg/cm²)	CV (%)	Mean ± SD (μg/cm²)	CV (%)	Mean ± SD (μg/cm²)	CV (%)	
Mg	0.231 ± 0.012	5.2	0.186 ± 0.009	4.8	0.279 ± 0.005	1.9	n.d.–0.0026
Al	0.235 ± 0.016	6.6	0.287 ± 0.019	6.7	0.420 ± 0.035	8.2	0.021–0.039
Si	0.914 ± 1.05	114.9	0.702 ± 0.159	22.7	1.071 ± 0.306	28.6	0.003–0.012
P	0.017 ± 0.008	48.2	0.026 ± 0.003	9.8	0.027 ± 0.004	14.6	0.001–0.003
S	3.420 ± 0.133	3.9	2.899 ± 0.077	2.6	6.219 ± 0.265	4.3	0–0.001
Cl	0.338 ± 0.022	6.5	0.355 ± 0.027	7.7	0.325 ± 0.017	5.4	n.d.
K	0.360 ± 0.039	10.7	0.931 ± 0.064	6.9	0.699 ± 0.018	2.6	n.d.–0.015
Ca	0.248 ± 0.007	2.9	0.314 ± 0.028	9.1	0.439 ± 0.052	11.9	0.01–0.032
Ti	0.031 ± 0.004	12.9	0.050 ± 0.008	16.4	0.059 ± 0.002	3.9	n.d.–0.007
V	0.010 ± 0.002	16.1	0.012 ± 0.003	29.0	0.013 ± 0.002	14.4	n.d.
Cr	0.009 ± 0.0015	13.3	0.014 ± 0.002	16.8	0.015 ± 0.002	14.3	n.d.–0.004
Mn	0.086 ± 0.008	8.8	0.080 ± 0.004	4.8	0.098 ± 0.005	5.2	n.d.
Fe	0.896 ± 0.044	4.9	1.382 ± 0.063	4.5	1.461 ± 0.060	4.1	0.013–0.022
Ni	0.033 ± 0.003	10.5	0.036 ± 0.001	3.4	0.036 ± 0.002	5.4	n.d.–0.041
Cu	0.080 ± 0.005	5.8	0.097 ± 0.003	3.1	0.088 ± 0.002	2.5	0.031–0.041
Zn	0.216 ± 0.013	5.9	0.276 ± 0.016	5.8	0.312 ± 0.008	2.6	n.d.–0.028

periods exceeded 20%. In this case, the CV of Si in the TSP samples in Table 3a confirmed that a sudden particle resuspension of large soil particles including Si might be collected on the filter. By excluding this accidental case, it was possible to collect five filter samples of $PM_{2.5}$ at the same quality in each sampling period, with CV of the elemental components with an air concentration of 50 ng/cm² or more falling within the range of about 15%

Table 4. Certified and measured values for SRM 2783 air particulate matter on filter (Zeisler *et al.*, 2006).

Element	Mass loading values on filter (μg)		CV of the measured value (%)	Difference of between certified and measured values (%)
	Certified	Measured		
Fe	26.50 ± 1.60	23.77 ± 0.83	2.9	−10.3
Al	23.21 ± 0.53	23.60 ± 0.43	1.8	1.7
Ca	13.20 ± 1.70	11.02 ± 0.34	3.1	−16.5
Mg	8.62 ± 0.52	5.70 ± 0.13	2.3	−33.9
K	5.28 ± 0.52	4.32 ± 0.25	5.3	−18.1
Zn	1.79 ± 0.13	1.79 ± 0.10	4.8	−0.3
Ti	1.49 ± 0.24	1.26 ± 0.08	5.1	−15.8
Cu	0.404 ± 0.042	0.62 ± 0.01	1.5	53.5
Mn	0.32 ± 0.012	0.27 ± 0.02	4.7	−16.9
Cr	0.135 ± 0.03	0.14 ± 0.02	10.1	3.7
Ni	0.068 ± 0.012	0.19 ± 0.02	8.9	185.9
V	0.049 ± 0.006	0.067 ± 0.035	48.9	38.1
Cl		1.65 ± 0.03	1.4	
P		0.89 ± 0.03	2.8	
	Reference			
Si	58.60 ± 1.60	55.89 ± 1.30	1.9	−4.6
S	1.05 ± 0.26	1.46 ± 0.05	3.4	39.2

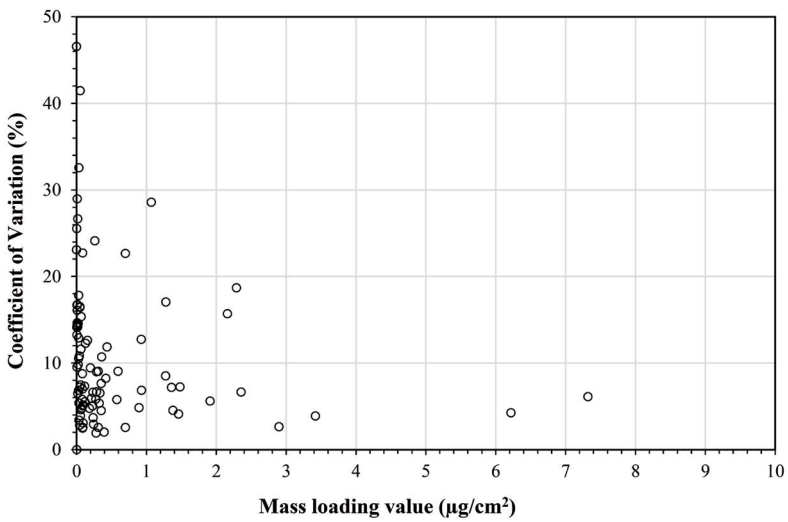

Fig. 12. Relationship between the average mass loading values on the filters and CV of simultaneously corrected TSP and $PM_{2.5}$ samples(n = 5) of each component.

or less in this study. In Table 3, the inorganic element components analysis results of the blank filters were shown. The slight excess of the CVs of Al, P, Ca, Ti, Cr, Fe, Ni, Cu in the TSP and $PM_{2.5}$ samples might be induced by large variation of the mass loading values in the blank filters of these elements, which were similar level of the concentration in the collected samples.

Table 4 shows certified and measured values for the standard material SRM2783 air particulate matter on filter. CV of repeated analysis of SRM2783 was less than 15% for Mg, Al, Si, P, S, Cl, K, Ca, Ti, Fe, Cr, Mn, Ni, Cu and Zn, and 49% for V. The EDXRF-FP method showed

Table 5. The approximate cost of SilVy-5 and similar sampler using flow meters instead of the critical nozzles.

No.	Details	Amount	Unit Price (JPY)	For SilVy-5 (JPY)	For sampler using flow meters (JPY)
1	Critical nozzle production	5	20,000	100,000	–
2	Valve for bypass	1	5,000	5,000	5,000
3	Filter holder	5	20,000	100,000	100,000
4	Impactor	5	50,000	250,000	250,000
5	Piping/Joints	1	20,000	20,000	20,000
6	Pump (DA-241S)	1	230,000	230,000	230,000
7	Flow meter (CMS0050)	5	150,000	–	750,000
8	Valve for flow control	5	5,000	–	25,000
	Total costs			705,000	1,380,000

good repeatability that was less than 15% of the target value except V. The deviation of four measured values from the certified value (Relative standard deviation) for SRM2783 was less than 15% for Al, Si, Cr, Fe and Zn, from 15% to 20% for K, Ca, Ti and Mn and greater than 30% for Mg, V, Ni, Cu and S. The concentrations of all other elements besides V in the SRM2783 sample were greater than 10 ng/cm^2 for the certified and measured values.

Fig. 12 shows the relationship between the average mass loading values on the filters and CV of simultaneously corrected $PM_{2.5}$ and TSP samples (n = 5) of each component. It is shown that the lower elemental mass loadings, the higher CV. In all EDXRF analyses, the X-ray from its source irradiates a sample, and detector counts (measures) incoming photons (radiation) to detect a peak of an element. A high concentration of an element emits more photons than a low concentration. Collecting more photons and hence increase the precision of detection. Also, the presence and concentrations of other elements influence the precision. The elements attenuate or enhance the number of emitted photons. Heavy elements absorb the greater part of the incoming radiation and the fluorescent radiation than light ones (Brouwer, 2010). However, ICP-MS or other higher sensitivity devices can further improve the measurement precision of each element.

3.3 Cost Calculation

The most important factors of the sampler for the wide and successful application are high measurement accuracy, low-cost and ease to use. The high costs of sampling devices of $PM_{2.5}$ in locations in developing countries limit comprehensive study of local and global air pollution. This has spurred researchers to develop low-cost samplers. We have created a simultaneous low volume air sampler using a critical nozzle. The sampler reduces the cost and simplifies hardware by replacing the flow meters with critical nozzles. The approximate cost of SilVy-5 produced in this study and compares it with a similar sampler using traditional flow meters (Table 5). According to the estimation, the manufacturing cost of SilVy-5 can be halved in compared to a sampler with similar performance that uses ordinary flow meters. Therefore, this is a great step in forwarding the ability to measure air quality in developing countries. The running cost of the sampler estimates pump working costs (electricity) the capital cost is very low due to the simple construction. For example, SilVy-5 never needs fixing or replacing the flowmeters or valves since it has not them at all. Moreover, optional costs, the calibrations and maintenances would not be required at beginning and during working processes.

4. CONCLUSIONS

We developed a low-cost multiple air sampling device to use in both developed and developing region such as the Central Asian countries. We use sonic venturi air flow devices to collect multiple $PM_{2.5}$ samples that can allow researchers to conduct multi-component analysis of aerosol compositions. According to experimental results, the constant airflow rate at 16.7 L/min was set with a backpressure ratio of 0.8 or less with a nozzle diameter of 1.375 mm. The sampler uses fewer mechanical devices and cuts costs by about half and simplifies the design by replacing the flow meters with critical nozzles.

Multiple samples were collected for 72 hours for TSP and $PM_{2.5}$, and 24 hours for TSP three times during three sampling periods to evaluate collection performance of sampler. For quantitative evaluation, CV of each component concentration of five samples was calculated and the variation was summarized. The CV of multi sample analysis for TSP and $PM_{2.5}$ concentrations in all sampling periods were less than 10%. CV of the major inorganic elements being within the range of 15% or less shows that the precision is sufficient for sampling for practical use. We believe that the low-cost multiple air sampler will be used world-widely, and it can contribute to many researchers in both developed and developing countries.

ACKNOWLEDGEMENT

Part of this research was supported by Tokyo Dylec Corp. and the Keio Leading-edge Laboratory Science and Technology Specified Research Projects, JSPS KAKENHI Grant Numbers JP17H04480, JP18K19856, JP20H00636, JST CREST JPMJCR19H3, the Environmental Research and Technology Development Fund by ERCA 5-2007, and Steel Foundation for Environmental Protection Technology. The research and studying of Zikrilla Alimov in the Ph.D. program at Keio University were supported by Japan International Cooperation Agency (JICA) according to the agreement between the governments of Uzbekistan and Japan on the Project for Strengthening the Capacity of Research in Uzbek-Japan Innovation Center of Youth (UJICY) at Tashkent State Technical University. The authors would like to thank Mr. Gray Horwitz for his support on English editing.

REFERENCES

Alam, M.M.A., Setoguchi, T., Matsuo, S., Kim, H.D. (2016) Nozzle geometry variations on the discharge coefficient. Propulsion and Power Research, 5(1), 22–33. https://doi.org/10.1016/j.jppr.2016.01.002

Amrani, D. (2013) A comparative study of sound speed in air at room temperature between a pressure sensor and a sound sensor. Physics Education, 48(1), 65. https://doi.org/10.1088/0031-9120/48/1/65

Atkinson, R.W., Fuller, G.W., Anderson, H.R., Harrison, R.M., Armstrong, B. (2010) Urban ambient particle metrics and health. A time series analysis. Epidemiology, 21, 501–5113. https://www.jstor.org/stable/25680581

Bonzini, M., Tripodi, A., Artoni, A., Tarantini, L., Marinelli, B., Bertazzi, P.A., Baccarelli, A. (2010) Effects of inhalable particulate matter on blood coagulation. Journal of Thrombosis and Haemostasis, 8(4), 662–668. https://doi.org/10.1111/j.1538-7836.2009.03694.x

Brouwer, P. (2010) Theory of XRF. Almelo, Netherlands: PANalytical BV. pp. 21–51.

Cadelis, G., Tourres, R., Molinie, J. (2014) Short-term effects of the particulate pollutants contained in Saharan dust on the visits of children to the emergency department due to asthmatic conditions in Guadeloupe (French Archipelago of the Caribbean). PLoS ONE, 9(3), e91136. https://doi.org/10.1371/journal.pone.0091136

Cohen, A.J., Ross, A.H., Ostro, B., Pandey, K.D., Krzyzanowski, M., Kunzli, N., Gutschmidt, K., Pope, A., Romieu, I., Samet, J.M., Smith, K. (2005) The Global Burden of Disease Due to Outdoor Air Pollution. Journal of Toxicology and Environmental Health, Part A, 68(13–14), 1301–1307. https://doi.org/10.1080/15287390590936166

Correia, A.W., Pope III, C.A., Dockery, D.W., Wang, Y., Ezzati, M., Dominici, F. (2013) The effect of air pollution control on life expectancy in the United States: an analysis of 545 us counties for the period 2000 to 2007. Epidemiology, 24(1), 23–31. https://doi.org/10.1097/EDE.0b013e3182770237

Fang, Y., Naik, V., Horowitz, L.W., Mauzerall, D.L. (2013) Air pollution and associated human mortality: the role of air pollutant emissions, climate change and methane concentration increases from the preindustrial period to present. Atmospheric Chemistry and Physics, 13, 1377–1394. https://doi.org/10.5194/acp-13-1377-2013

Huang, Y.C., Ghio, A.J. (2006) Vascular Effects of Ambient Pollutant Particles and Metals. Current Vascular Pharmacology, 4(3), 199–203. https://doi.org/10.2174/157016106777698351

ISO 9300:2005 (2005) Measurement of gas flow by means of critical flow Venturi nozzles.

JIS Z 8767:2006 (2006) Measuring method of gas flow rate using critical venturi nozzle (CFVN).

JIS Z 8851:2008 (2008) Sampler of $PM_{2.5}$ in ambient air.

Johnson, R.C. (1965) Real-gas effects in critical-flow-through nozzles and tabulated thermodynamic properties (Vol. 2565). National Aeronautics and Space Administration. pp. 4–7.

Kim, K.H., Kabir, E., Kabir, S. (2015) A review on the human health impact of airborne particulate matter. Environment international, 74, 136–143. https://doi.org/10.1016/j.envint.2014.10.005

Kumar, A., Gupta, T. (2015) Development and laboratory performance evaluation of a variable configuration $PM_1/PM_{2.5}$ impaction-based sampler. Aerosol and Air Quality Research, 15(1), 768–775. https://doi.org/10.4209/aaqr.2014.11.0307

Kunzli, N., Tager, I.B. (2005) Air Pollution from Lung to Heart. Swiss Medical Weekly, 135(47–48), 697–702.

Lim, S.S., Vos, T., Flaxman, A.D., Danaei, G., Shibuya, K., Adair-Rohani, H., Aryee, M. (2012) A comparative risk assessment of burden of disease and injury attributable to 67 risk factors and risk factor clusters in 21 regions, 1990–2010: a systematic analysis for the Global Burden of Disease Study 2010. The Lancet, 380(9859), 2224–2260. https://doi.org/10.

1016/S0140-6736(12)61766-8
Mannucci, P.M., Franchini, M. (2017) Health effects of ambient air pollution in developing countries. International Journal of Environmental Research and Public Health, 14(9), 1048. https://doi.org/doi.org/10.3390/ijerph14091048
Meister, K., Johansson, C., Forsberg, B. (2012) Estimated short-term effects of coarse particles on daily mortality in Stockholm, Sweden. Environmental Health Perspectives, 120(3), 431–436. https://doi.org/10.1289/ehp.1103995
MOEGJ (Ministry of the Environment, Government of Japan) Quality control commentary, May 2019. http://www.env.go.jp/air/manual_0.pdf
Morioka, T., Nakao, S., Ishibashi, M. (2011) Characteristics of critical nozzle flow meter for measuring high-pressure hydrogen gas. The Japan Society of Mechanical Engineers, Volume B, 7(776), 1088–1096 (in Japanese). https://doi.org/10.1299/kikaib.77.1088
Nakahara Ward Office, Kawasaki City Government (NWOKCG) (2020) http://sc.city.kawasaki.jp/taiki/DOWNLOAD/Y2019.html
Nakamura, K., Naung, K.T., Monji, H. (2014) Study on Supersonic Nozzle Flow with Micro Bubbles. Journal of the Japanese Society for Experimental Mechanics, 14(Special_Issue), s88–s93. https://doi.org/10.11395/jjsem.14.s88
Nakao, S.I., Yokoi, Y., Takamoto, M. (1996) Development of a calibration facility for small mass flow rates of gas and the uncertainty of a sonic venturi transfer standard. Flow Measurement and Instrumentation, 7(2), 77–83. https://doi.org/10.1016/S0955-5986(97)00006-X
Okuda, T., Isobe, R., Nagai, Y., Okahisa, S., Funato, K., Inoue, K. (2015) Development of a high-volume $PM_{2.5}$ particle sampler using impactor and cyclone techniques. Aerosol and Air Quality Research, 15(3), 759–767. https://doi.org/10.4209/aaqr.2014.09.0194
Okuda, T., Schauer, J.J., Shafer, M.M. (2014) Improved methods for elemental analysis of atmospheric aerosols for evaluating human health impacts of aerosols in East Asia. Atmospheric Environment, 97, 552–555. https://doi.org/10.1016/j.atmosenv.2014.01.043
Sabyrbekov, R., Ukueva, N. (2019) Transitions from dirty to clean energy in low-income countries: insights from Kyrgyzstan. Central Asian Survey, 38(2), 255–274. https://doi.org/10.1080/02634937.2019.1605976
Sapkota, P., Bastola, U. (2017) Foreign direct investment, income, and environmental pollution in developing countries: Panel data analysis of Latin America. Energy Economics, 64, 206–212. https://doi.org/10.1016/j.eneco.2017.04.001
Sharma, R.K., Agrawal, M. (2005) Biological Effects of Heavy Metals: An Overview. Journal of Environmental Biology, 26(2), 301–313.
Treesubsuntorn, C., Dolphen, R., Dhurakit, P., Siswanto, D., Thiravetyan, P. (2017) Green technology innovation in a developing country. AIP Conference Proceedings 1908, 030004. https://doi.org/10.1063/1.5012704
Viana, M., Querol, X., Alastuey, A., Gil, J.I., Menéndez, M. (2006) Identification of PM sources by principal component analysis (PCA) coupled with wind direction data. Chemosphere, 65(11), 2411–2418. https://doi.org/10.1016/j.chemosphere.2006.04.060
Wang, X., Zhang, Y. (1999) Development of a critical airflow venturi for air sampling. Journal of Agricultural Engineering Research, 73(3), 257–264. https://doi.org/10.1006/jaer.1999.0414
Wang, X., Zhang, Y., Zhao, L., Riskowski, G.L. (1999) Development of a multipoint aerosol sampler using critical flow control devices. ASHRAE Transactions, 105, 1108–1113.
Wong, G.S. (1990) Approximate equations for some acoustical and thermodynamic properties of standard air. Journal of the Acoustical Society of Japan (E), 11(3), 145–155. https://doi.org/10.1250/ast.11.145
Younglove, B.A., Frederick, N.V. (1992) Speed-of-sound measurements in liquid and gaseous air. International Journal of Thermophysics, 13(6), 1033–1041. https://doi.org/10.1007/BF01141213
Zeisler, R., Murphy, K.E., Becker, D.A., Davis, W.C., Kelly, W. R., Long, S.E., Sieber, J.R. (2006) Standard Reference Materials® (SRMs) for measurement of inorganic environmental contaminants. Analytical and Bioanalytical Chemistry, 386(4), 1137–1151. https://doi.org/10.1007/s00216-006-0785-7